

CHAPTER IV

THEORETICAL STUDY ON AN ABSORPTION SPECTRA FOR CHROMOPHORES

Rhodamine and acridine families are the fluorescent dye. Upon absorbing light, they instantly emit light at a longer wavelength than the light absorbed. They are detected as a different color. Many fluorophores can be conjugated to other molecules without significant alteration of their photophysical properties. Fluorescent probes enable researchers to detect particular components of complex biomolecular assemblies, including live cells, with exquisite sensitivity and selectivity.

The fluorophores possess a conjugated π electron system, which mainly determines its spectral properties. The energy term scheme of the molecules with a conjugated π electron system is illustrated by a Jablonksi diagram in Figure 4.1. A photon of energy is supplied by an external source such as an incandescent lamp or a laser and absorbed by the fluorophore (A), creating an excited singlet states (S). This process distinguishes fluorescence from chemiluminescence, in which the excited state is populated by a chemical reaction.

When the molecule is excited to the first (S1) or higher singlet states, the molecule can relax to the ground state either via the internal conversion (IC) or by emitting a fluorescence photon from S1 state (F). However, not all the molecules initially excited by absorption return to the ground state S0 by fluorescence emission (F). Other processes such as collisional quenching, Fluorescence Resonance Energy Transfer (FRET), blinking, and intersystem crossing may also depopulate S1. The fluorescence quantum yield (QY), which is the ratio of the number of fluorescence photons emitted (F) to the number of photons absorbed (A), is a measure of the extent to which these processes occur.

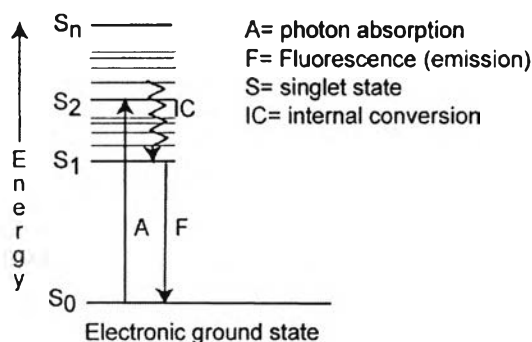


Figure 4.1. Energy term scheme.

The biological interest in acridine results primarily from its chromophore properties. The electronic spectra of acridines have been investigated by several authors. Jean and Nounir have studied the influence of solvent polarity on the electronic absorption of selected acridine derivatives. [94] Kunlhiko and co-worker have investigated excited acridine, deuterated acridine and 9-substitued acridines in acidic water that showed absorption at 400 nm^{-1} . [95] Moreover, Stephan and co-worker presented spectra for 9-aminoacridine with aluminosilicate xerogel glasses, with absorption maxima at 380, 400 and 422 nm. [96] Óscar and co-workers have studied the electronic absorption spectra of acridine computationally by multistate CASPT2.[97]

Moreover, we studied rhodamine 6G which is an excellent laser or Forensic Light Source dye. It can be dissolved in water or solvents to be used as a liquid dye in solution staining, or it can be introduced into magnetic powder to form a fluorescent magnetic powder. Rhodamine fluorophores are useful in biological research because of their brightness or and photophysical property.

Rhodamine 6G (R6G) is also called rhodamine 590 chloride. The chemical name of this dye is: 2-[6(ethylamino)-3-(ethylimino-2,7-dimethyl-3H-xanthen-9-yl)]-benzoic acid, ethyl ester, monohydrochloride with a formula of: $\text{C}_{27}\text{H}_{29}\text{O}_3\text{N}_2 \cdot \text{HCl}$. The absorption maximum wavelength of R6G is 530 nanometers [98,99] and the fluorescence emission maximum wavelength is 560 nanometers

The applications in our study involve covalent attachment of the dye such as rhodamine and aminoacridine to DNA and the charge transport dynamics of

intercalated organic dyes. This study is a prerequisite to understanding the excited-state properties of chromophore intercalated in DNA.

Aim of this chapter is to investigate the electronic spectra of the chromophores. The investigations were carried out in the gas phase and in aqueous solution.

4.1 Models and methods

Unconstrained geometry optimizations of chromophore were carried out at AM1 level of theory. Geometries for derivatives of aminoacridine and R6G were optimized at the B3LYP/6-31G* level with Gaussian98 program. We also investigated Fragment 1 (pyronine 6G) and Fragment 2 of R6G (see Figure 4.4) which were optimized by B3LYP/6-31G*.

Excitation energies and oscillator strengths were calculated using configuration interaction of selected singly excited states with the semiempirical, AM1, NDDO-G methods. The excited state properties were calculated using the configuration interaction method (CI). 100 singly excited states were taken into account (all single excitations from ten occupied and to ten virtual orbitals). The calculations were carried out with the program SIBIQ [100] in the gas phase and in implicit water model. Moreover, the absorption spectra are investigated in gas phase using TDDFT calculations at B3LYP/6-31G* level with Gaussian98.

4.2 Results and discussions

4.2.1 Acridine

The electronic spectra calculating using a acridine molecule was started. It is the simplest dye compared to others. The geometry optimization of the ground state of acridine was performed with the AM1 method imposing C_{2v} symmetry constraints. The optimized geometric parameters are listed in Table 4.1. The calculated C-C bond lengths of acridine by AM1 were compared with X-ray values and CASSCF results. In general, calculated and available experiment structures do not differ much.

The maximum deviation, C5-C6, is 0.016 Å between AM1 calculation and experiment data.

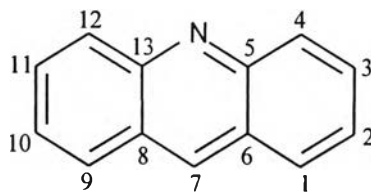


Table 4.1 Selected optimized structure parameters of acridine obtained from the AM1 and CASSCF calculation in comparison with experiment (distances in Å, angles in degrees).

parameters	AM1	CASSCF [97]	Expt. [101]
C1-C2	1.361	1.358	1.364
C2-C3	1.426	1.439	1.420
C3-C4	1.365	1.341	1.376
C4-C5	1.446	1.440	1.434
C5-C6	1.441	1.421	1.425
C6-C7	1.367	1.393	1.382
C6-C1	1.429	1.436	1.435
C5-N	1.367	1.332	-
C1-H1	1.101	1.075	-
C2-H2	1.101	1.074	-
C3-H3	1.101	1.074	-
C4-H4	1.101	1.074	-
C7-H7	1.102	1.076	-
C2C1C6	120.7	120.5	-
C2C1H1	121.3	120.7	-
C6C1H1	118.1	118.8	-
C2C3C4	121.2	120.8	-
C3C4C5	120.6	120.8	-
C4C5C6	118.8	118.8	-
C4C5N	119.7	118.3	-
C6C7H7	120.1	120.2	-

Table 4.2 Excitation energies (E), wavelengths (λ) and oscillator strengths (f) of acridine obtained at semiempirical level of theory and CIS with 100 CI in gas phase.

state	NDDO-G			AM1			INDO/S			CASPT2 [97]	Expt. [101]
	E	λ	f	E	λ	F	E	λ	f		
1B ₂	3.569	347.4	0.00894	3.240	382.6	0.00153	3.554	348.8	0.04397	3.58	3.5
2A ₁	3.778	328.2	0.19659	3.288	377.1	0.07564	3.764	329.4	0.18528	3.77	-
1B ₁	3.675	337.4	0.00000	3.785	319.9	0.00000	3.852	321.9	0.00000	3.87	-
2B ₂	4.799	258.3	0.31837	4.236	292.7	0.02844	4.866	254.8	0.03038	4.59	4.6

Table 4.2 lists the spectra of acridine at the optimized AM1 geometry. We consider the four lowest state, involving transitions among valence orbitals: 1B₂ at 3.569, 3.240 eV and 3.554; 2A₁ at 3.778, 3.785 and 3.764 eV; 1B₁ at 3.675, 3.288 and 3.853 eV and 2B₂ 4.799, 4.236 and 4.866 eV for NDDO-G, AM1 and INDO/S, respectively.

Overall, the results are quite good at NDDO-G calculation. The NDDO-G energy results do not differ substantially from previously report calculated using more sophisticated techniques. However, the 1A₁ energy is larger than 2B₁ energy that is different from CASPT2 method. The absorption spectrum of acridine has been changes when solvent effect is included. The 2B₁ excitation energy is greater than 1A₁ energy (Table 4.3). The differences in excitation energies calculated in the gas phase and in aqueous solution are 0.03, 0.04, 0.37 and 0.04 for 1B₂, 2A₁, 1B₁ and 2B₂, respectively. Furthermore, the results of AM1 method yield lower excitation energies when compare with CASPT2 calculation and experiment. For the INDO/S calculation, the excitation energy of 2A₁ agree with NDDO-G, yet the oscillator strength of 2B₂ is lower than NDDO-G.

Table 4.3 Excitation energies (E), wavelengths (λ) and oscillator strengths (f) of acridine in water obtained at NDDO-G and CIS with 100 CI.

State	E(eV)	λ (nm)	f
1B ₂	3.603	344.1	0.02559
2A ₁	3.743	331.2	0.18915
1B ₁	4.042	306.7	0.00000
2B ₂	4.755	260.7	0.00681

The molecule is in the xy plane and belongs to the point group C_{2v} . We have defined C_2^x axis passing through nitrogen and opposite carbon atom. Inspection of Figure 4.2 as the highest occupied molecular orbital (HOMO) has been gone into negative under a C_2^x axis and xy plane, from a basis for b1 representation. It has been presented in Lowest unoccupied molecular orbital (LUMO) as well (See Appendix).

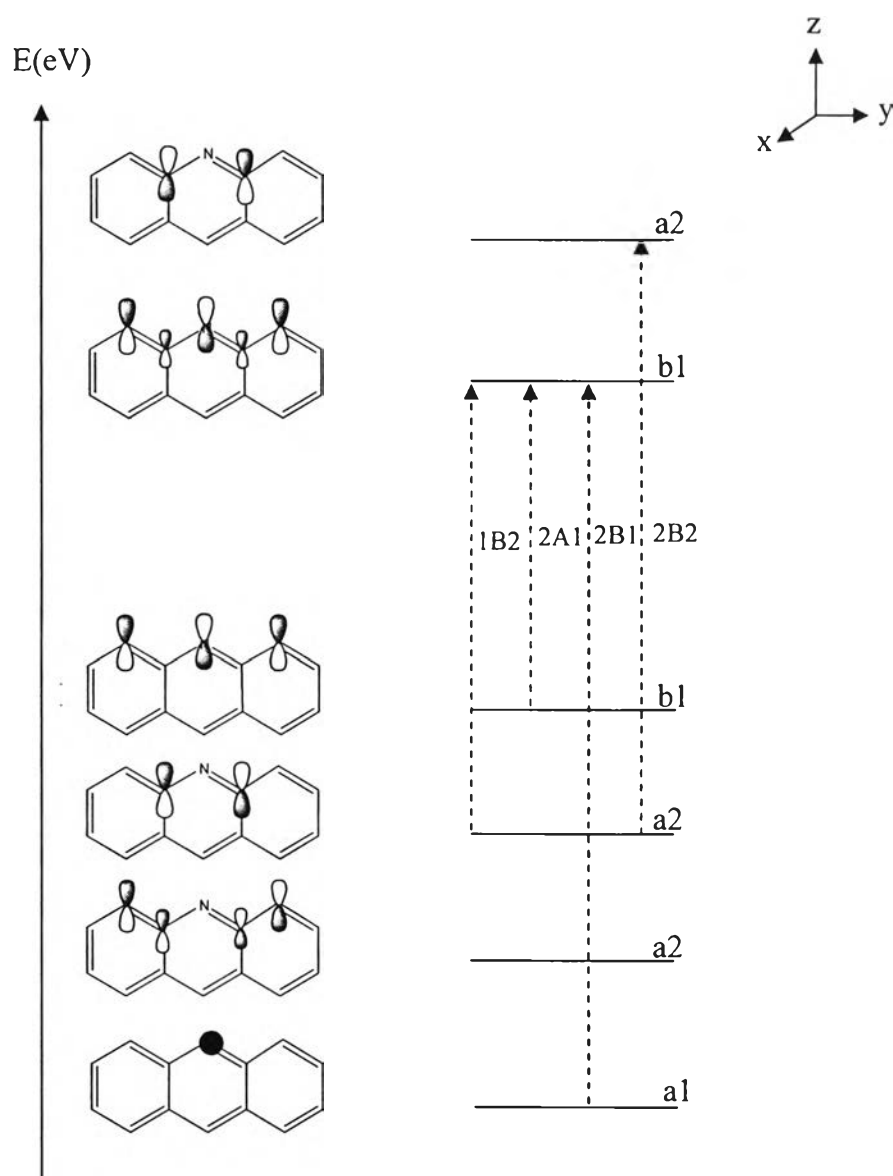


Figure 4.2 Highest occupied and lowest unoccupied molecular orbitals labels

The important electronic transitions occur between four highest occupied and two lowest virtual orbitals (see Figure 1.). The transition to $1B_2$ and $2A_1$ states can be related to the 1L_b and 1L_a bands of Platt's model, respectively. The $2A_1$ state involves excitations between the one high-lying occupied orbital and the one low-lying unoccupied orbital, which described as HOMO \rightarrow LUMO as the topology of HOMO (b1) and LUMO (b1). As regards the $1B_2$ state described as HOMO-1 \rightarrow LUMO when HOMO-1 is a2. These results agree well with MS-CASPT2 calculation.

4.2.2 Aminoacridine derivatives

The structures of aminoacridine derivative with $R = CH_3$ and H were fully optimized. The corresponding geometries are shown in Table 4.4. The parameters of the two derivatives do not differ significantly; the largest change, only 0.014 Å, was calculated for the distance C7-C8.

Geometries optimized with the AM1 method are close to those calculated with B3LYP. The maximum difference of 0.002 Å was found for C5-N. However, the DFT calculations require much more time.

Aminoacridine derivatives in the gas phase and in aqueous solution were studied. According to our calculations, the first excitation energies, of aminoacridine derivatives in the gas phase are slightly different (see Table 4.5). The excitation can be related to transition between the highest occupied orbital and the lowest unoccupied orbital labeled as HOMO \rightarrow LUMO. In aqueous solution, the difference in energy was found to be 0.058 eV when changing CH_3 by H. The spectroscopic properties of $R = H$ is quite different from the results of a calculations with the time dependent DFT method, based on B3LYP/6-31G*. The first absorption energy shifts by 29.5 nm (409.9 vs. 439.4 nm for AM1 and TD DFT, respectively). Oscillator strengths also differ by about 50% which are 0.119 and 0.077 for AM1 and TDDFT, respectively.

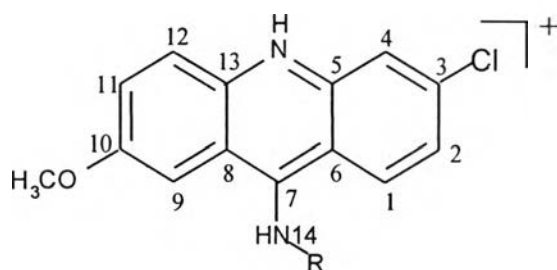


Table 4.4 Selected optimized parameter for structure of aminoacridine derivatives (Å) obtained at the B3LYP/6-31G* level

Parameter	R = CH3	R = H
C1-C2	1.375	1.373
C2-C3	1.412	1.416
C3-C4	1.379	1.378
C4-C5	1.409	1.411
C5-C6	1.428	1.423
C6-C7	1.441	1.434
C6-C1	1.426	1.423
C5-N	1.364	1.365
C7-C8	1.457	1.443
C8-C9	1.410	1.414
C9-C10	1.390	1.384
C10-C11	1.417	1.417
C11-C12	1.379	1.376
C12-C13	1.408	1.410
C13-C8	1.418	1.421
C13-N	1.374	1.372
N-H	1.013	1.013
C10-O	1.349	1.352
C7-N14	1.340	1.340

Table 4.5 Excitation energies (E), wavelengths (λ) and oscillator strengths (f) of aminoacridine derivatives in the gas phase and water obtained with AM1 (CIS with 100 states) and TDDFT methods.

	Gas phase				Water		
	R	E	λ	f	E	λ	f
AM1	CH ₃	3.003	412.8	0.1783	3.118	397.7	0.2312
	H	3.030	409.9	0.1198	3.176	390.4	0.2086
TDDFT	H	2.822	439.4	0.0765	-	-	-

In addition, the electronic properties of aminoacridine derivatives were investigated in aqueous solution. The calculated absorption energies were found to be blue-shifted by 0.115 and 0.146 eV for R = CH₃ and H, respectively.

When comparing to experiment, it was found that the absorption of R = H differ from the available experiment by 0.005 and 0.151 eV for the calculations in gas phase and water, respectively. The experiment absorption maximum of ACMA was observed at 3.025 eV (the measurement was carried out in buffer containing 1% ethanol at 20 °C). [102]

4.2.3 Rhodamine 6G

First, let us consider the results in the gas phase calculations. The first state involves excitations between the one highest occupied orbital and the one lowest unoccupied orbital, which described as HOMO→LUMO

Table 4.6 lists of spectra of rhodamine 6G (R6G) at optimized structure. The first excitation energies of R6G in gas phase are 457.6, 438.5, 425.4 nm for AM1, NDDO-G and time dependent method with B3LYP/6-31G*, respectively.

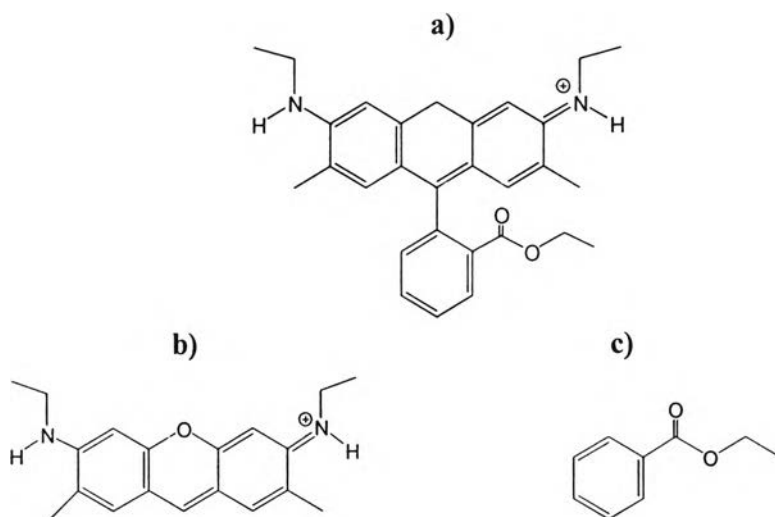


Figure 4.3 Structure of a) R6G, b) Fragment 1(pyronine 6G) and c) Fragment 2

Table 4.6 Excitation energies (E), wavelengths (λ) and oscillator strengths (f) in gas phase obtained at semiempirical level of theory (CIS with CI 100 state) and TDDFT calculation.^a

Molecule	State	AMI			NDDO-G			TDDFT		
		E(eV)	λ (nm)	f	E(eV)	λ (nm)	f	E(eV)	λ (nm)	f
R6G	1	2.710	457.6	0.882	2.828	438.5	1.051	2.915	425.4	0.757
	2	3.215	385.6	0.001	3.443	360.1	0.011	3.258	380.6	0.000
	3	3.612	343.3	0.076	3.934	315.1	0.000	3.696	335.5	0.152
	4	3.894	318.4	0.112	4.046	306.5	0.057	3.724	333.0	0.003
Fragment 1	1	2.612	474.7	0.902	2.727	454.6	1.094	2.862	433.2	0.824
	2	3.170	391.1	0.005	3.331	372.2	0.008	3.164	392.2	0.000
	3	3.568	347.5	0.083	3.965	312.7	0.036	3.942	314.5	0.043
	4	3.971	312.2	0.177	4.191	295.9	0.004	4.015	308.8	0.003
Fragment 2	1	3.910	317.1	0.006	4.480	276.8	0.008	-	-	-
	2	4.139	299.6	0.017	4.789	258.9	0.000	-	-	-
	3	4.264	290.7	0.000	5.506	225.2	0.271	-	-	-
	4	5.833	212.6	0.895	6.339	195.6	0.857	-	-	-

^a The R6G structure has been optimized using B3LYP/6-31g*.

The spectroscopic properties of R6G are quite different from the experimental result. The first absorption energy shifts by 72.4, 91.5 and 104.6 nm for AM1, NDDO-G and TDDFT, respectively. The absorption maximum wavelength of R6G is 530 nanometers.

As the Table 4.1, the absorption spectrum of R6G was compared with those of Fragments 1 and 2, which the structure of Fragment 1 is the pyronine 6G molecule. (see Figure 4.3) The three lowest states at AM1 level of theory were considered: the first state at 457.6, 474.7 and 317.1 nm, the second state at 385.6, 391.1 and 299.6 nm and the third state at 343.3, 347.5 and 290.7 nm for R6G, Fragment 1 and Fragment 2, respectively. The spectrum of R6G is near to the Fragment 1 more than Fragment 2.

Analysis of excitation localization at AM1 level of theory is shown in Table 4.7. The results agree with those in Table 4.6. In the first three states, electron delocalization of 98% was found in F1 and a few percent between F1 and F2 (see Figure 4.4 and Table 4.7). It was found that the first electron delocalization of about 68.9 % in F2 at the fourth state. There is 13.2 % of electron delocalization from F1 to F2 and 15 % from F2 to F1 in this state. At the next state, electron delocalization is only 5.2 % in F2 but 59.6 % in F1. Moreover, the large delocalization of electrons from F2 to F1 of about 96.5 % and 92.3% were found in the eighth and tenth states, respectively.

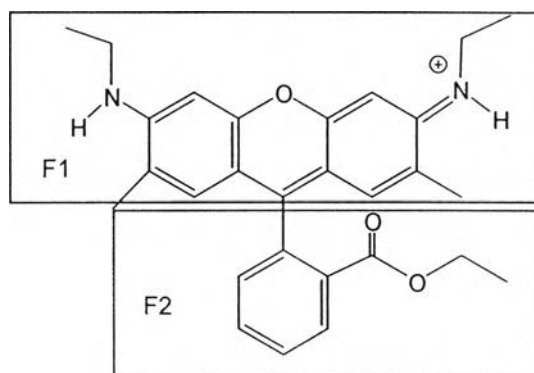


Figure 4.4 The regions F1 and F2 of the R6G.

In addition, the electronic properties of R6G were studied in aqueous solution. (see Table 4.8) The AM1 and NDDO-G calculated adsorption peaks are at 466.3 and 437.4 nm (the first excited state), 385.2 and 359.2 nm (the second excited state), 343.7 and 306.2 nm (the third excited state) and 320.8 and 294.6 nm (the fourth excited state).

The differences in the wavelengths calculated in the gas phase and in water are 8.7 nm (475.6 vs. 466.3 nm) and 1.1 nm (438.5 vs. 437 nm) for AM1 and NDDO-G level of theory, respectively. The absorption spectra in water yielded from the AM1 and NDDO-G differ from the available experiment by 64 and 93 nm, respectively. The experiment absorption maximum of R6G was observed at 530 nm (the measurement was carried out in ethanol).

Table 4.7 AM1 calculations of the electronic spectrum of R6G and fragment analysis of excitation localization.^a

State	E(eV)	λ (nm)	f	Excitation delocalization (%)			
				F1→F1	F2→F2	F1→F2	F2→F1
1	2.710	457.6	0.882	98.2	0.0	1.6	0.2
2	3.215	385.6	0.001	97.4	0.0	1.4	1.2
3	3.612	343.3	0.077	98.1	0.0	1.0	0.9
4	3.894	318.4	0.112	2.9	68.9	13.2	15.0
5	3.977	311.7	0.221	59.6	5.2	17.4	17.8
6	4.151	298.7	0.152	95.0	0.1	2.6	2.4
7	4.249	291.8	0.011	1.7	75.4	10.7	12.2
8	4.285	289.4	0.000	1.9	1.6	0.0	96.5
9	4.547	272.7	0.378	84.7	0.6	6.9	7.7
10	4.575	271.0	0.000	6.1	1.5	0.1	92.3

^a The R6G structure has been optimized using B3LYP/6-31g*.

Table 4.8 Excitation energies (E), wavelengths (λ) and oscillator strengths (f) of R6G in water obtained with AM1 (CIS with 100 states).^a

State	AM1			NDDO-G		
	E(eV)	λ (nm)	f	E(eV)	λ (nm)	f
1	2.659	466.3	0.923	2.853	437.4	1.057
2	3.219	385.2	0.005	3.452	359.2	0.017
3	3.608	343.7	0.060	4.040	306.2	0.040
4	3.865	320.8	0.160	4.208	294.6	0.003

^a The R6G structure has been optimized using B3LYP/6-31g*.

Several models were constructed by varying the substituent (R1 and R2) (See Figure 4.5). The calculated spectra of the models are reported in Table 4.9. The absorption spectra of R6G are slightly different from model 1 by 3.7 and 5.1 for model 2 and 2.1 and 0.5 nm for model 3 with AM1 and NDDO-G calculation, respectively. The model 2 was built by replacing $-\text{CH}_3$ (R2) with H. The model 3 was made by changing $-\text{C}_2\text{H}_5$ (R1) to CH_3 . Furthermore, the absorption spectra of model 4 were dramatically blue shift by 25.4 nm when compared with model 1. (wavelengths: at AM1; 457.6 and 432.2 nm and at NDDO-G: 438.5 and 423.5 nm for model 1 and model 3, respectively) This model was constructed by varying both R1 and R2.

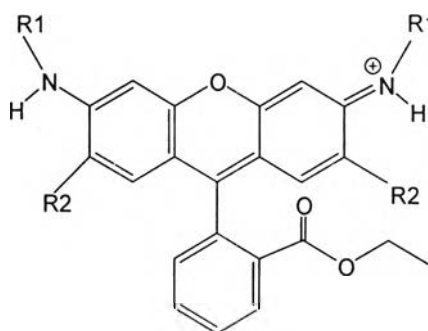


Figure 4.5 Varying the substituent R1 and R2 on R6G.

Table 4.9 Comparison of the excitation energies (E), wavelengths (λ) and oscillator strengths (f) of R6G models in gas phase obtained at semiempirical level of theory and CIS with CI 100 state.^a

Model	R1	R2	AM1			NDDO-G		
			E(eV)	λ (nm)	f	E(eV)	λ (nm)	f
1	C ₂ H ₅	CH ₃	2.710	457.6	0.882	2.828	438.5	1.051
2	C ₂ H ₅	H	2.731	453.9	0.890	2.861	433.4	1.052
3	CH ₃	CH ₃	2.697	459.7	0.866	2.824	439.0	1.052
4	CH ₃	H	2.869	432.2	0.857	2.928	423.5	1.017

^a The R6G structure has been optimized using B3LYP/6-31g*.

The deprotonation energy, the energy of the proton transfer from RH⁺ to a water molecule:



is shown in Table 4.10. It is defined as

$$\text{deprotonation energy} = [\text{E}(\text{R}) + \text{E}(\text{H}_3\text{O}^+)] - [\text{E}(\text{RH}^+) + \text{E}(\text{H}_2\text{O})].$$

The deprotonation energies of 94.0 and 22.5 kcal/mol for the gas phase and water are rather large. The result suggest that deprotonation state of R6G is unlikely to be formed both in the gas phase and water solution.

Table 4.10 Calculation deprotonation energies of R6G at AM1 level of theory

Molecule	Heat of formation (kcal/mol)	
	Gas phase	Water
unprotonated (M)	-16.0	-34.5
H ₃ O ⁺	143.5	45.4
protonated (MH ⁺)	92.7	53.9
H ₂ O	-59.3	-65.5
deprotonation energy	94.0	22.5



4.3 Conclusion

The first excited energy of the acridine is found to be 3.569 eV. at the NDDO-G method. The difference of the absorption energy between acridine and aminoacridine derivatives predicted at AM1 level of theory amount to 0.1 eV. The absorption spectra were observed to be change when solvent effects are included.

The parameters of acridine calculated with AM1 are in agreement with those obtained at the high level of theory, CASSCF. However, the results of AM1 method yield lower excitation energies which are less accurate when compare with multistate CASPT2 calculation and experiment.

We calculated excitation energies of R6G with the TDDFT, AM1 and NDDO-G methods. The calculated excitation energies overestimate the experiment value in all cases. The best agreement was found for the AM1 (the difference is 72.4 nm).

Analysis of excitation localization at AM1 level of theory was shown that electron delocalization of 98% was found in F1 and a few percent between F1 and F2.

The solvent environment was found to influence weakly on the excitation of R6G. Moreover, our calculations on the deprotonation energy of R6G have revealed that the molecule should be protonated in water solution.

The NDDO-G method has an advantage for the calculation of the first excited state of molecules. This method is not only accurate enough, but also saves computational time. The qualitative conclusion would not be changed by the use of the sophisticated calculation.